

Pseudogap behavior of RuP probed by photoemission spectroscopy

K. Sato¹, D. Ootsuki², Y. Wakisaka¹, N. L. Saini^{3,1}, T. Mizokawa^{1,2}, M. Arita⁴,
H. Anzai⁴, H. Namatame⁴, M. Taniguchi^{4,5}, D. Hirai⁶, and H. Takagi^{2,6}

¹*Department of Complexity Science and Engineering,*

University of Tokyo, 5-1-5 Kashiwanoha, Chiba 277-8561, Japan

²*Department of Physics, University of Tokyo, 5-1-5 Kashiwanoha, Chiba 277-8561, Japan*

³*Department of Physics, University of Roma "La Sapienza" Piazzale Aldo Moro 2, 00185 Roma, Italy*

⁴*Hiroshima Synchrotron Radiation Center, Hiroshima University, Higashi-hiroshima 739-0046, Japan*

⁵*Graduate School of Science, Hiroshima University, Higashi-hiroshima 739-8526, Japan and*

⁶*Department of Advanced Materials, University of Tokyo, 5-1-5 Kashiwanoha, Chiba 277-8561, Japan*
(Dated: November 13, 2018)

We have studied the electronic structure of RuP and related Ru pnictides using photoemission spectroscopy. Ru *3d* core-level and valence-band spectra of RuP show that the Ru valence is +3 with t_{2g}^5 configuration. The photoemission spectral weight near the Fermi level is moderately suppressed in the pseudogap phase of RuP, consistent with the pseudogap opening of $2\Delta/k_B T_c \sim 3$ (gap size $\Delta \sim 50$ meV and transition temperature $T_c \sim 330$ K). The Ru *3d* peak remains sharp in the pseudogap phase and the insulating phase of RuP, suggesting that the electronic orderings responsible for the phase transitions are different from the conventional charge density wave.

PACS numbers: 74.70.Xa, 74.25.Jb, 71.30.+h, 71.20.-b

Intensive and extensive research activities have been dedicated to understand the electronic phase diagram of Fe pnictide family since the discovery of superconductivity and magnetism in $\text{LaFeAsO}_{1-x}\text{F}_x$.^{1,2} The Fe pnictide superconductors show an interesting interplay between superconductivity and magnetism which is similar to cuprate superconductors. In the case of the cuprate superconductors, pseudogap behavior is believed to be one of the key ingredients to understand the relationship between the superconductivity and the magnetism. On the other hand, pseudogap behavior has never been established in the Fe pnictide superconductors although it was claimed in an early photoemission study.³ Very recently, Hirai *et al.* have discovered that Ru pnictides have a unique electronic phase diagram with insulating, superconducting, and pseudogap phases.⁴ This has opened up a new opportunity to study the relationship between superconductivity and pseudogap in the pnictides. Ru pnictides have a complicated three-dimensional structure (MnP-type structure) as schematically shown in Fig. 1 and shows a transition from a metal to a non-magnetic insulator. Transitions from metals to non-magnetic (or almost non-magnetic) insulators have been reported in various transition-metal compounds including pyrochlore-type $\text{Ti}_2\text{Ru}_2\text{O}_7$,^{5,6} spinel-type CuIr_2S_4 ,^{7,8} LiRh_2O_4 ,⁹ MgTi_2O_4 ,^{10,11} hollandite-type $\text{K}_2\text{V}_8\text{O}_{16}$.^{12,13} However, superconductivity has not been realized in any of these by destroying the non-magnetic insulating phases. In this context, the non-magnetic insulating phase of RuP is very interesting and important since the superconductivity is induced by Rh doping.⁴ The electric resistivity of RuP takes a minimum at $T_1 = 330$ K with a drastic increase due to the metal-to-insulator transition around $T_2 = 270$ K. The magnetic susceptibility of RuP shows Pauli paramagnetic behavior above T_1 and gradually decreases below T_1 with an almost discontinuous

drop around T_2 to a negative value which is comparable to the expected core diamagnetism.⁴ This suggests that RuP is a normal metal above T_1 and a non-magnetic insulator below T_2 . In the temperature range between T_1 and T_2 , RuP shows the pseudogap behavior. RuAs resembles RuP with $T_1 = 280$ K and $T_2 = 200$ K while RuSb is a normal metal down to the lowest temperature. In this paper, we report core-level and valence-band x-ray photoemission spectroscopy (XPS) and valence-band ultraviolet photoemission spectroscopy (UPS) of RuP and related Ru pnictides. While XPS provides information on the fundamental electronic structure of Ru^{3+} (t_{2g}^5) in RuP, spectral evidence of pseudogap opening is obtained by UPS measurement of RuP.

Polycrystalline samples of RuP, $\text{Ru}_{0.75}\text{Rh}_{0.25}\text{As}$, and RuSb were prepared as reported in ref. 4.⁴ The XPS measurements were performed using a JPS-9200 spectrometer equipped with a monochromatized Al $K\alpha$ x-ray source ($h\nu = 1486.6$ eV). The total energy resolution was 600 meV. The base pressure of the spectrometer was in the 1.0×10^{-7} Pa range. The UPS measurements were performed using SES-100 analyzer with the He I line ($h\nu = 21.2$ eV). The total energy resolution was 30 meV. The base pressure of the spectrometer was 5.0×10^{-8} Pa. The high-energy resolution UPS measurements have been performed at beamline 9A at Hiroshima Synchrotron Radiation Center (HiSOR). The photon energy from the normal incidence beamline was set to $h\nu = 10$ eV. The total energy resolution was 8 meV. The binding energy was calibrated using the Fermi edge of the gold reference sample. The base pressure of the chamber was 2.0×10^{-9} Pa. The polycrystalline samples of RuP were fractured in situ at 300 K in order to obtain clean surfaces for the XPS and UPS measurements.

Figure 2 shows the Ru *3d* core level XPS spectra of RuP measured at 300 K and 40 K which are compared

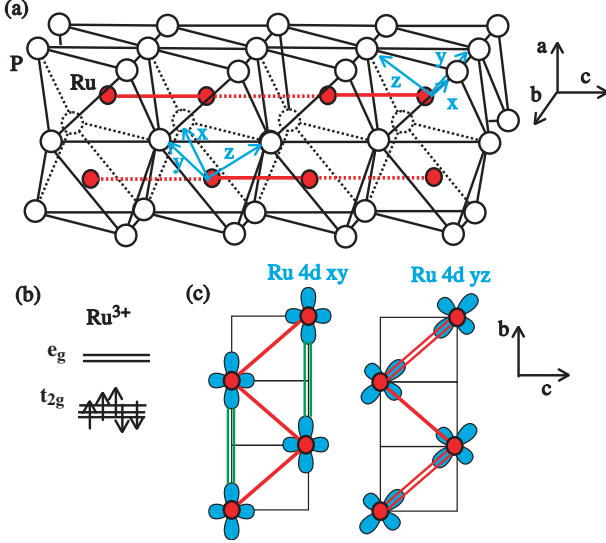


FIG. 1: (color online) (a) Schematic drawing for crystal structure of RuP. The RuP₆ octahedra share their edges and faces to form the three-dimensional structure. The distortion of RuP₆ octahedron is neglected and the shift of Ru ions are included. The shorter (longer) Ru-Ru bonds are indicated by the solid (dashed) lines. (b) Electronic configurations of Ru³⁺ (t_{2g}^5). (c) Ru 4d t_{2g} orbitals on the zig-zag double chain formed by the shorter Ru-Ru bonds. In case of Ru 4d xy or yz orbital ordering, the Ru-Ru dimers are formed as indicated by the double lines.

with the Ru 3d core level XPS spectrum of Sr₂Ru⁴⁺O₄ at 300K.¹⁴ The Ru 3d_{5/2} peaks of RuP and Sr₂RuO₄ are located at 280 eV and 281 eV, respectively. The difference of the Ru 3d binding energy is consistent with difference of Ru valence between trivalent RuP and tetravalent Sr₂Ru⁴⁺O₄. Therefore, the Ru³⁺ in RuP takes t_{2g}^5 electronic configuration with $S = 1/2$. Thus, the mechanism of the metal-to-insulator transition of RuP should be different from that of Tl₂Ru₂O₇ with t_{2g}^4 electronic configuration.⁶ The Ru 3d_{5/2} peaks of RuP at 300 K and 40 K are rather narrow and do not change appreciably across the metal-to-insulator transition at 270 K. If the metal-to-insulator transition is driven by charge density wave (CDW) formation, the Ru 3d peak of the CDW phase is expected to be broadened or be split due to the Ru 4d charge modulation just like the observations in TaS₂¹⁵ and CuIr₂S₄.¹⁶ However, the Ru 3d_{5/2} peak of the insulating phase is narrow and is essentially the same as that of the metallic phase, indicating that there is no CDW or that the magnitude of charge modulation, if exists, is very small.

Figure 3(a) shows the valence-band XPS ($h\nu = 1486.6$ eV) and UPS ($h\nu = 10$ eV) spectra of RuP taken at 300 K. The broad structures ranging from the Fermi level (E_F) to 2.5 eV are derived from the Ru 4d t_{2g} orbitals hybridized with the P 3p orbitals. The near- E_F spectrum below 1.0 eV is featureless while the spectral features at 1.4 eV, 1.9 eV, and 2.2 eV are clearly observed. Since

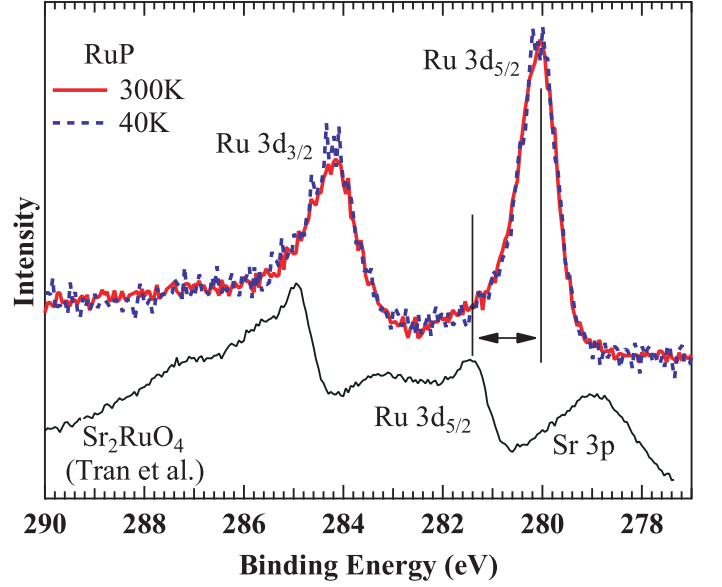


FIG. 2: (color online) Ru 3d core-level XPS photoemission spectra of RuP taken at 300 K and 40 K compared with that of Sr₂RuO₄ by Tran *et al.*¹⁴

Ru 4d photo-ionization cross section relative to P 3p increases from 10 eV to 1486.6 eV, the spectral weight from E_F to 1.0 eV has stronger Ru 4d character than that from 1 eV to 2.5 eV. In Figs. 3(b) and (c), the near- E_F UPS spectrum of RuP taken at 300 K is compared with that of Ru_{0.75}Rh_{0.25}As and RuSb. In Fig. 3(c), the photoemission spectra are divided by Fermi distribution functions for each temperature convoluted with a Gaussian function of FWHM of 8 meV. The spectral weight from E_F to ~ 50 meV is suppressed in RuP compared to those of Ru_{0.75}Rh_{0.25}As and RuSb. This spectral weight suppression is consistent with the pseudogap phase of RuP between $T_1 = 330$ K and $T_2 = 270$ K. The energy scale of pseudogap $\Delta \sim 50$ meV is roughly consistent with the pseudogap transition temperature $T_c \sim 330$ K since the $2\Delta/k_B T_c$ value is ~ 3 close to the BCS value.

Figure 4(a) shows the near- E_F UPS spectra of RuP taken at 300K, 230K, 120K and 40K at $h\nu = 10$ eV. They are normalized to the integrated spectral weight from 0.2 eV to -0.1 eV. Across the metal-to-insulator transition temperature, the spectral weight at E_F does not decrease in spite of the metal-to-insulator transition. This indicates that the surface region of RuP remains metallic even when the bulk undergoes the metal-to-insulator transition. Although the main part of the surface-sensitive UPS spectrum does not represent the interesting phase transition of the bulk, the electronic structural change of the bulk can be picked up in the UPS spectra as discussed below. In order to identify the spectral change at E_F , the photoemission spectra are divided by Fermi distribution functions for each temperature convoluted with a Gaussian function of FWHM of 8 meV. In Fig. 4(b), the data up to $3k_B T$ above E_F are plot-

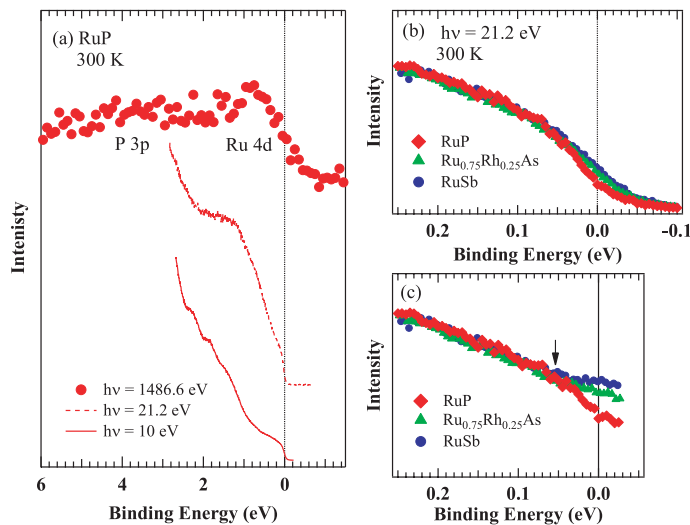


FIG. 3: (color online) (a) Valence-band XPS and UPS spectra of RuP taken at 300 K. (b) Near- E_F photoemission spectrum of RuP compared with those of $\text{Ru}_{0.75}\text{Rh}_{0.25}\text{As}$ and RuSb. (c) Near- E_F photoemission spectra divided by Fermi distribution functions for each temperature convoluted with a Gaussian function of FWHM of 8 meV.

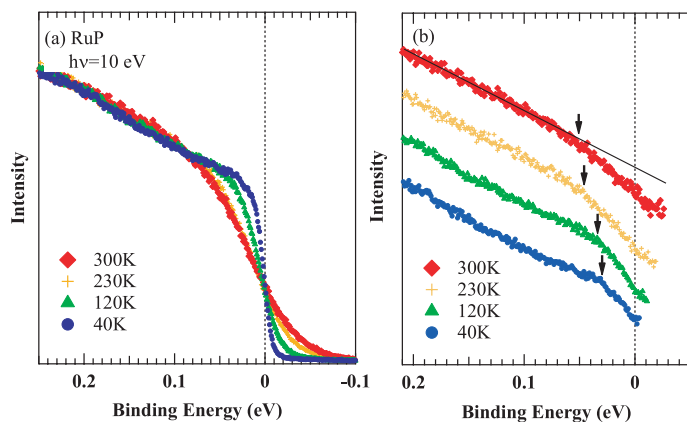


FIG. 4: (color online) (a) Near- E_F photoemission spectra of RuP taken at 300 K, 230 K, 120 K, and 40 K. (b) Near- E_F photoemission spectra of RuP divided by Fermi distribution functions for each temperature convoluted with a Gaussian function of FWHM of 8 meV.

ted where reasonably good signal-to-noise ratio is available. The spectral weight below ~ 50 meV is suppressed at 300K indicating the pseudogap opening of ~ 50 meV. Interestingly, the magnitude of pseudogap apparently decreases with cooling. Although the full gap opening as-

sociated with the metal-to-insulator transition is not observed probably due to the metallic surface, we speculate that the order parameter of the pseudogap phase is competing with that of the insulating phase.

Here, we propose a possible interpretation for the two successive transitions of RuP using the idea of the orbitally-induced Peierls mechanism.¹⁷ In the transition from the normal metal to the pseudogap phase at $T_1 = 330$ K, since the suppression of the magnetic susceptibility is moderate, a kind of band Jahn-Teller effect or an orbital order of the Ru $4d$ t_{2g} bands is expected to produce quasi-one-dimensional Fermi surfaces by the Ru $4d$ xy orbitals [see the left panel of Fig. 1(c)]. In this orbital order, the neighboring Ru $4d$ xy electrons tend to form spin-singlet dimers along the b-axis which can explain the suppression of the magnetic susceptibility. However, the Fermi surfaces with the Ru $4d$ yz and zx characters remain below T_1 . The transition from the pseudogap phase to the insulating phase at $T_2 = 270$ K can be assigned to another kind of band Jahn-Teller effect or an orbital order to lift the degeneracy of yz and zx orbitals [see the right panel of Fig. 1(c)]. The metal-insulator transition at T_2 is driven by the Peierls transition of the quasi-one-dimensional Fermi surfaces formed by the Ru $4d$ yz or zx orbital. This scenario could be consistent with the fact that the two transitions of RuP at $T_1 = 330$ K and $T_2 = 270$ K show different responses to the Rh doping.⁴ While T_2 disappears very rapidly in the underdoped region, the pseudogap transition temperature T_1 remains around room temperature up to the optimum doping level where the superconducting transition temperature of $\text{Ru}_{1-x}\text{Rh}_x\text{P}$ reaches maximum.

In conclusion, we have studied the electronic structure of RuP using XPS and UPS. Ru $3d$ core-level and valence-band spectra of RuP show that the Ru valence is +3 with t_{2g}^5 configuration. Since the Ru $3d$ core-level peak remains sharp in the pseudogap phase and the insulating phase of RuP, the electronic orderings responsible for the phase transitions are different from the conventional charge density wave. The photoemission spectral weight near the Fermi level is moderately suppressed in the pseudogap phase of RuP. The energy scale Δ of the spectral weight suppression is ~ 50 meV, indicating $2\Delta/k_B T_c \sim 3$. It is argued that the two successive transitions at T_1 and T_2 in RuP would correspond to the Peierls-like transitions in xy and yz/zx orbital channels, respectively.

The authors would like to thank valuable discussions with D. I. Khomskii. The synchrotron radiation experiment was performed with the approval of HSRC (Proposal No.11-A-7).

¹ Y. Kamihara, T. Watanabe, M. Hirano, and H. Hosono, J. Am. Chem. Soc. **130**, 3296 (2008).

² H. Takahashi, K. Igawa, K. Arii, Y. Kamihara, M. Hirano, and H. Hosono, Nature **453**, 376 (2008).

³ Y. Ishida, T. Shimojima, K. Ishizaka, T. Kiss, M. Okawa,

T. Togashi, S. Watanabe, X.-Y. Wang, C.-T. Chen, Y. Kamihara, M. Hirano, H. Hosono, and S. Shin, Phys. Rev. B **79**, 060503(R) (2009).

⁴ D. Hirai, T. Takayama, D. Hashizume, and H. Takagi, Phys. Rev. B **85**, 140509(R) (2012).

- ⁵ H.S. Jarrett, A.W. Sleight, J.F. Weiher, J.L. Gillson, C.G. Frederick, G.A. Jones, R.S. Swingle, D. Swartzfager, J.E. Gulley, P.C. Hoell, *Valence Instabilities and Related Narrow-Band Phenomena*, p. 545 (Plenum, New York, 1977).
- ⁶ S. Lee, J.-G. Park, D. T. Adroja, D. Khomskii, S. Streltsov, K. A. McEwen, H. Sakai, K. Yoshimura, V. I. Anisimov, D. Mori, R. Kanno and R. Ibberson, *Nature Mat.* **5**, 471 (2006).
- ⁷ S. Nagata, N. Matsumoto, Y. Kato, T. Furubayashi, T. Matsumoto, J. P. Sanchez and P. Vulliet, *Phys. Rev. B* **58**, 6844 (1998).
- ⁸ P. G. Radaelli, Y. Horibe, M. J. Gutmann, H. Ishibashi, C. H. Chen, R. M. Ibberson, Y. Koyama, Y. S. Hor, V. Kirykhin, and S. W. Cheong, *Nature* **416**, 155 (2002).
- ⁹ Y. Okamoto, S. Niitaka, M. Uchida, T. Waki, M. Takigawa, Y. Nakatsu, A. Sekiyama, S. Suga, R. Arita, and H. Takagi, *Phys. Rev. Lett.* **101**, 086404 (2008).
- ¹⁰ M. Isobe and Y. Ueda, *J. Phys. Soc. Jpn.* **71**, 1848 (2002).
- ¹¹ M. Schmidt, W. Ratcliff, P.G. Radaelli, K. Refson, N.M. Harrison, and S.W. Cheong, *Phys. Rev. Lett.* **92**, 056402 (2004).
- ¹² M. Isobe, S. Koishi, N. Kouno, J. Yamaura, T. Yamauchi, H. Ueda, H. Gotou, T. Yagi, and Y. Ueda, *J. Phys. Soc. Jpn.* **75**, 073801 (2006).
- ¹³ A. C. Komarek, M. Isobe, J. Hemberger, D. Meier, T. Lorenz, D. Trots, A. Cervellino, M. T. Fernandez-Diaz, Y. Ueda, and M. Braden, *Phys. Rev. Lett.* **107**, 027201 (2011).
- ¹⁴ T. T. Tran, T. Mizokawa, S. Nakatsuji, H. Fukazawa, and Y. Maeno, *Phys. Rev. B* **70**, 153106 (2004).
- ¹⁵ K. Horiba, K. Ono, J. H. Oh, T. Kihara, S. Nakazono, M. Oshima, O. Shiino, H. W. Yeom, A. Kakizaki, and Y. Aiura, *Phys. Rev. B* **66**, 073106 (2002).
- ¹⁶ K. Takubo, S. Hirata, J. Y. Son, J. W. Quilty, T. Mizokawa, N. Matsumoto, and S. Nagata, *Phys. Rev. Lett.* **95**, 246401 (2005).
- ¹⁷ D. I. Khomskii and T. Mizokawa, *Phys. Rev. Lett.* **94**, 156402 (2005).